AD-A066 250 MASSACHUSETTS INST OF TECH LEXINGTON LINCOLN LAB F/G 20/3
LOCAL SITE DISTORTION MODEL OF MAGNETOSTRICTION.(U)
NOV 78 G F DIONNE
UNCLASSIFIED TR-532 ESD-TR-78-292 F19628-78-C-0002 NL

1 OF 1
ADA
066250

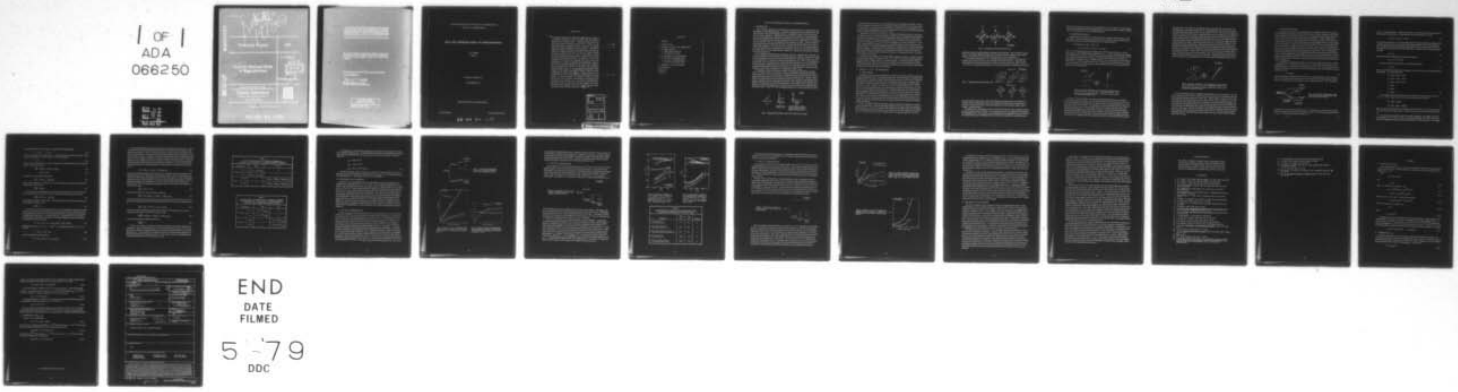

END
DATE
FILMED
5-79
DDC

Technical Report 532

Local Site Distortion Model of Magnetostriction

G. F. Dionne

29 November 1978

Prepared for the Department of the Army
under Electronic System Division Contract F19628-78-C-0002 by

Lincoln Laboratory
MASSACHUSETTS INSTITUTE OF TECHNOLOGY
Lexington, Massachusetts

The work reported in this document was performed at Lincoln Laboratory, a center for research operated by Massachusetts Institute of Technology. This program is sponsored by the Ballistic Missile Defense Program Office, Department of the Army; it is supported by the Ballistic Missile Defense Advanced Technology Center under Air Force Contract F19628-78-C-0002.

This report may be reproduced to satisfy needs of U.S. Government agencies.

This technical report has been reviewed and is approved for publication.

FOR THE COMMANDER

Raymond L. Loiselle, Lt. Col., USAF
Chief, ESD Lincoln Laboratory Project Office

MASSACHUSETTS INSTITUTE OF TECHNOLOGY
LINCOLN LABORATORY

LOCAL SITE DISTORTION MODEL OF MAGNETOSTRICTION

G. F. DIONNE
Group 33

TECHNICAL REPORT 532

29 NOVEMBER 1978

LEXINGTON MASSACHUSETTS

ABSTRACT

A new model is proposed to explain the magnetostriction effects in ferrimagnetic spinels and garnets with Mn^{3+}, Co^{2+}, and Fe^{2+} ions substituted into octahedral sites. Considerable experimental evidence has revealed that small amounts of each of these ions will alter substantially the magnitude of either the λ_{100} or λ_{111} magnetostriction constant, depending on the particular ion. The theory is based on the concept that Jahn-Teller effects produce local site distortions of tetragonal (favoring $\langle 100 \rangle$ axes) or trigonal (favoring $\langle 111 \rangle$ axes) symmetry which are able to switch among the different axes of the particular family in order to select the axis closest to the direction of the magnetic field. For Mn^{3+} ions, the local site distortions are expected to be tetragonal ($c/a > 1$), in accord with observations in a variety of magnetic oxides where static cooperative effects are present, and will produce large positive changes in the λ_{100} constant. With Co^{2+} ions, the distortion is also tetragonal, but of the opposite sign ($c/a < 1$), consistent with cooperative effects in CoO, and will produce large negative changes in λ_{100}. In the case of Fe^{2+} ions, the distortion is trigonal ($\alpha < 60°$), as evidenced by its behavior in FeO, and will produce large positive changes in the λ_{111} constant. In each case studied, the theoretical results are in complete accord with the available room temperature magnetostriction constant data on a qualitative basis. An estimate of the magnitude of the elastic energy of the local site distortion suggests that crystal field energy level splittings required to create the observed magnetostrictive effects are only on the order of .01 cm^{-1}.

CONTENTS

LOCAL SITE DISTORTION MODEL OF MAGNETOSTRICTION

I. INTRODUCTION

When a material undergoes an elastic deformation upon application of a magnetic field, the phenomenon is called magnetostriction. In general, this property exists in spontaneously magnetic materials, such as ferromagnetic metals or ferrimagnetic oxides, where trivalent iron (Fe^{3+}) is found in abundance. Magnetostrictive distortions are measured as strains along the direction of the magnetization and feature a saturation curve which varies with field strength, as well as the hysteresis and remanent effects associated with the magnetization. For materials of cubic symmetry, there are two magnetostriction constants (λ_{100} and λ_{111}) which represent the saturation strains resulting when the field is directed along the $\langle 100 \rangle$ and $\langle 111 \rangle$ axes of a single-crystal specimen. Pure materials with an abundance of iron or other magnetic element will feature magnetostriction arising from the cooperative effects of the iron and its coupling to the crystal lattice, and the magnetostriction constants are considered to characterize this basic property of the material.

In ferrimagnetic compounds of spinel and garnet structure, magnetostriction constants can be severely affected by small quantities of selected transition-metal ions. The type of ion which creates this phenomenon is either crystal-field stabilized from a Jahn-Teller effect, e.g., Mn^{3+} in an octahedral site, or Jahn-Teller and spin-orbit stabilized, e.g., Co^{2+} in an octahedral site. In both cases, the ion itself is the source of a spontaneous distortion of its local environment. The large changes in magnetostriction constants can occur when these ions replace Fe^{3+} ions in substitution amounts of less than one percent and can be used effectively to control the magnitudes and signs of these constants over a considerable range of values.

Ferrimagnetic compounds with these ions have found important applications in memory cores, microwave devices, and may also be useful in controlling stress sensitivity of bubble memory materials. For the host material, the magnetostriction constants arise from the competing interactions between the crystal electric field and the magnetic field. Through a Stark effect, the crystal field will tend to break down the spin-orbit coupling by capturing the orbital angular momentum, while the spin angular momentum remains aligned with the magnetic field. However, the decoupling of the spin-orbit interaction is never complete and a small amount of spin-lattice coupling is always present to produce lattice strains whenever the magnetic field is rotated (see Fig. 1). Since Fe^{3+} is the predominant magnetic ion in these materials, and since

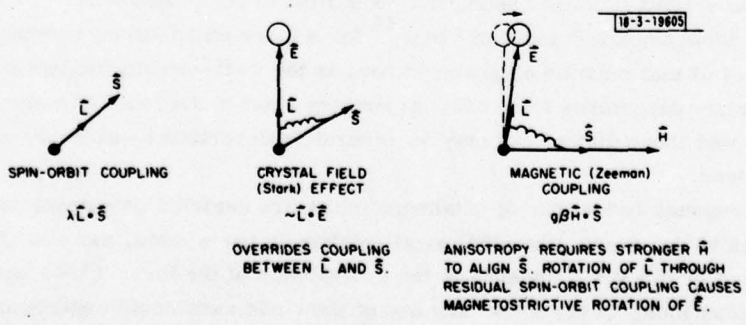

Fig. 1. Magnetoelastic effects and the role of spin-orbit coupling.

it is an S-state ion with no first-order contributions to the orbital angular momentum, even its collective magnetostriction effects are very small, seldom greater than a few parts per million. As a consequence, it is reasonable to assume that the contributions to the magnetostriction effects from these substituted ions are not only totally dominant, but may also be largely unaffected by the spin-lattice interactions of the host Fe^{3+} ions.

Although there are several ions that may be capable of producing these effects, this paper will examine only three for which an abundance of experimental and theoretical studies have been carried out. In particular, Mn^{3+} has been investigated in yttrium iron garnet[1] and in spinels (Li and Mg ferrite),[2-4] Co^{2+} has been examined in yttrium iron garnet[5] and in spinels (Li and Mg ferrite, and magnetite),[6,7] and Fe^{2+} has been investigated in yttrium iron garnet.[8-11] In all cases, magnetostriction constants λ_{100} and λ_{111} change monotonically with the amount of substitution of the particular ion and the effect is present at all temperatures at which measurements have been reported. In addition to the overall changes in magnetostriction constants, there are also the unheralded observations that in each situation one constant is affected more severely than the other, and both the affected constant and the sign of the change appear to be a property of the particular ion involved.

In an effort to gain insight into the origin of these important phenomena, a simple model has been developed to explain the behavior of Mn^{3+}, Co^{2+}, and Fe^{2+} in situations where substitution amounts are small enough to ignore any cooperative effects. Predictions of magnetostrictive changes based on this model are shown to be in complete accord with experiment on a qualitative basis, and totally consistent with theoretical predictions of the type of distortion anticipated for these ions in octahedral oxygen coordinations.

II. THEORY OF LOCAL SITE DISTORTIONS

A. Basic Concepts

Crystal-field and spin-orbit coupling effects are capable of creating reductions in symmetry of ligand coordinations with certain transition-metal ions. More specifically, in octahedral and tetrahedral sites, tetragonal or trigonal distortions may take place in order to lower the ground-state energy of the cation. One such case is the Jahn-Teller effect (static or dynamic) which often involves a simple tetragonal distortion or a combination of tetragonal and orthorhombic distortions in order to permit the crystal field to split a degenerate ground state. In situations where some orbital degeneracy still remains after all crystal field distortions have taken place, spin-orbit coupling will stabilize the ion. Without burdening this text with theoretical explanations of the origins of these phenomena, it is best to refer the reader to the writings of Goodenough,[12,13] Slonczewski,[14] and Van Vleck,[15] for a more complete background on this subject. The only result that must be emphasized here is the well-established fact that in all of the cases of interest, departures from cubic symmetry exist in the local environment of the individual ions and that these distortions may be accurately described by sketches of octahedral oxygen coordinations.

In Fig. 2, tetragonal distortions of octahedral sites are depicted as extensions or compressions of the length of the c axis (the [001] axis) relative to the a axes, and are characterized by the ratio $c/a > 1$ or $c/a < 1$. Because of the equivalence of the three $\langle 100 \rangle$ axes through the three-fold symmetry along $\langle 111 \rangle$ axes, any one of the cubic axes could experience this distortion. In a simple cubic lattice where isolated events of this type may take place, the local

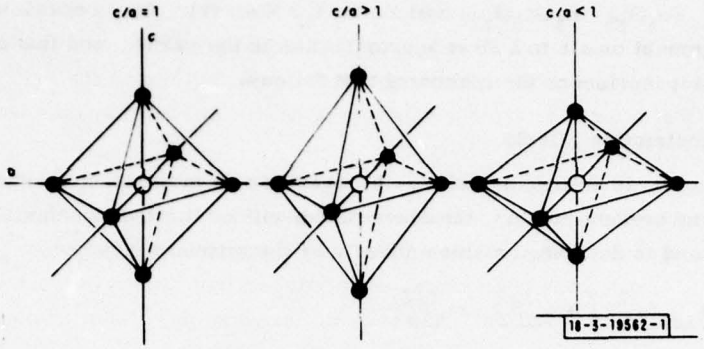

Fig. 2. Tetragonally distorted octahedral sites.

distortions would be divided statistically among the three directions. With increases in concentration, a cooperative distortion along one of the directions would eventually cause a phase change, and the symmetry of the crystal would switch from cubic to tetragonal.

For a trigonally distorted site, i.e., distortion along a body diagonal or $\langle 111 \rangle$ axis, the situation may be seen more clearly with a trigonal unit cell shown in Fig. 3. Extensions and compressions of the dimension along the [111] axis are characterized by the angle $\alpha > 60°$ or $\alpha < 60°$, and are reflected as shear strains in the associated octahedra. Because of the four-fold

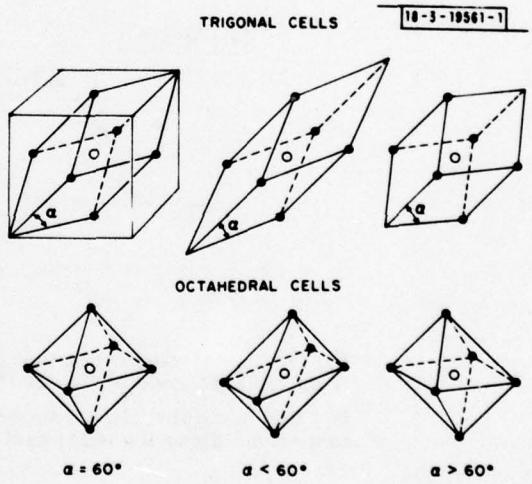

Fig. 3. Trigonally distorted octahedral sites.

symmetry along the cubic axes, all four body diagonals are equally likely to be subjected to a distortion and the individual distortions would be statistically distributed among these four directions in a simple cubic lattice, unless concentrations are large enough to create a phase change to trigonal symmetry.

In a spinel lattice, the octahedral site is oriented with its axes in perfect alignment with the principal symmetry axes of the lattice. For the garnet structure, the alignment is not identical, but reasonably close. The results of X-ray crystallographic investigations by Euler and Bruce[16] have shown that the axes of octahedral sites are within a few degrees of the symmetry axes of

the lattice for $Y_3Fe_5O_{12}$, $Y_3Ga_5O_{12}$, and $Y_3Al_5O_{12}$ (Ref. 17). As a result, it will be assumed that perfect alignment exists to a first approxi nation in the garnet, and that a model of a simple cubic lattice is appropriate in the reasoning that follows.

B. Magnetostriction Effects

Magnetostriction is defined as the strain imparted to a material when subjected to a magnetic field. In the present context, the phenomenon will be limited to uniaxial strains from a saturating field and is described mathematically by the standard equation

$$\lambda = \frac{3}{2}\lambda_{100}(\alpha_1^2\beta_1^2 + \alpha_2^2\beta_2^2 + \alpha_3^2\beta_3^2 - \frac{1}{3}) + 3\lambda_{111}(\alpha_1\alpha_2\beta_1\beta_2 + \alpha_2\alpha_3\beta_2\beta_3 + \alpha_3\alpha_1\beta_3\beta_1) \quad (1)$$

where λ is the magnetostrictive strain along an axis with direction cosines β_1, β_2, and β_3; λ_{100} and λ_{111} are the magnetostriction constants; and α_1, α_2, and α_3 are the direction cosines of the magnetic field. In Eq. (1), it should be noted that when the field is directed along a $\langle 100 \rangle$ axis, the strain along the [100] axis is λ_{100}; when the field is rotated to the [111] axis, the strain along the [100] axis is zero. In the same fashion, the strain along the [111] axis changes from zero to λ_{111} for the same rotation of field. Therefore, direct measurement of λ_{100} and λ_{111} can be carried out by determining the changes along these respective axes as the field direction is rotated between them.

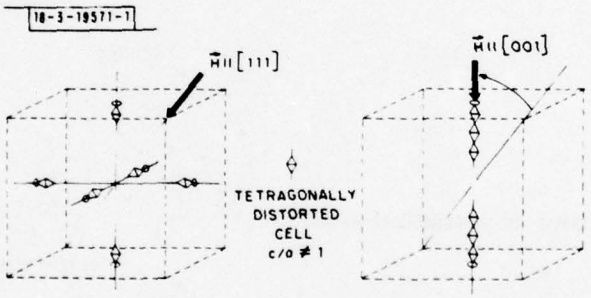

Fig. 4. Local site distortion ($c/a \neq 1$) switching as $\vec{H}$ is rotated from the [111] axis to the [001] axis. Diagram is intended to convey that each site aligns distortion axis with $\vec{H}$ to create a resultant strain along the [001] axis.

In Fig. 4, the case of a simple cubic crystal containing distributed sites with tetragonal ($c/a \neq 1$) distortions is considered. With the magnetic field directed along the [111] axis, there is no preferred direction of distortion for the isolated sites, and an equal distribution over each of the three $\langle 100 \rangle$ axes will result. This situation is required to preserve the basic symmetry elements of the cubic lattice. The net result would be an equal strain along each cubic axis, producing a slight change in the crystal lattice parameter. Consider now what should happen when the field is rotated to the [001] direction. Because of the residual spin-lattice interaction existing with each of the individual sites, a preferential alignment along the magnetic field axis will result in a net magnetostrictive strain along the [001] axis, as each site distortion switches

to this direction. The essence of this argument may be understood from Fig. 1, where it is demonstrated how a minimum energy state will be established when $\vec{E}$, the axial crystal electric field component becomes collinear with the magnetic field $\vec{H}$. Thus, when $\vec{H}$ is rotated between the [111] and [001] directions, a magnetostrictive strain (corresponding to the addition of local site distortions from two-thirds of the substituted ions) should appear along the [001] direction, smaller strains of the opposite sign (resulting from the loss of one-third of the distortions) should appear along the [100] and [010] directions, and no first-order change should be detected along the [111] axis. This last conclusion is based on a symmetry argument: if the distortions are small enough that the combined strain along the [001] direction does not alter the basic cubic symmetry of the lattice, the effects of the individual tetragonal distortions on the total [111]-axis strain will be independent of how these distortions are distributed among the three $\langle 100 \rangle$ directions. In other words, the switching of two-thirds of the distorted-sites to the [001] direction will have no first-order effect on the $\langle 111 \rangle$ axes strains, because each of these axes is centro-symmetric to the three cubic axes. Tetragonally distorted sites should produce changes in the λ_{100} magnetostriction constant without any significant effects on λ_{111}.

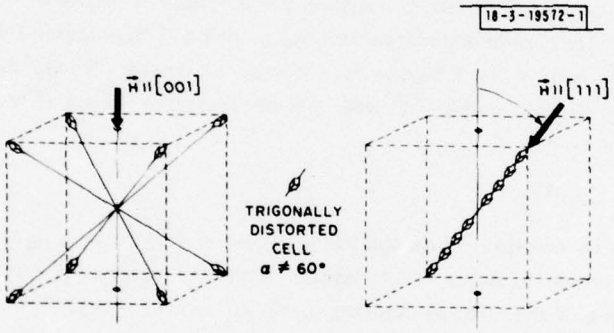

Fig. 5. Local site distortion ($\alpha \neq 60°$) switching as $\vec{H}$ is rotated from the [001] axis to the [111] axis. Diagram is intended to convey that each site aligns distortion axis with $\vec{H}$ to create a resultant strain along the [111] axis.

In Fig. 5, the analogous case of trigonally distorted sites ($\alpha \neq 60°$) is presented. Here the reverse situation occurs. With the field directed along a $\langle 100 \rangle$ axis, the individual sites align their trigonal distortions along the four $\langle 111 \rangle$ axes. When the field is rotated to the [111] axis, three-quarters of the distorted sites switch to that particular direction, producing a net [111]-axis strain that is four times greater than the original. By the same symmetry argument used in the case of the tetragonal distortions, it may be reasoned that strains along the $\langle 100 \rangle$ axes are insensitive to the directions of the magnetic field because these axes are centro-symmetric to the four $\langle 111 \rangle$ axes. The first-order effect of any individual trigonally distorted cell on the strain along the $\langle 100 \rangle$ axes will be independent of the particular $\langle 111 \rangle$ axis of the distortion. Trigonally distorted sites should thus produce changes in the λ_{111} constant without any appreciable effect on λ_{100}.

C. Stress-Strain Concepts

If ϵ^{S}_{100} refers to the strain along a $\langle 100 \rangle$ axis of a tetragonally distorted site and ϵ^{S}_{111} to the strain along a $\langle 111 \rangle$ axis of a trigonally distorted site, a lattice containing N sites would undergo magnetostrictive strains $\Delta\lambda_{100}$ or $\Delta\lambda_{111}$, depending on the type of distorted sites involved. Since the origins of these site strains are deformations of oxygen ligands about a crystal-field stabilized ion, the corresponding site stresses σ^{S}_{100} and σ^{S}_{111} will be determined by the balance between the crystal-field stabilization energy and the increase in elastic energy of the crystal lattice. According to the Jahn-Teller theorem,[18-20] an ion with an orbitally degenerate ground state will interact with the crystal electric field to produce a splitting of the degeneracy and a corresponding distortion in the crystal field by means of a localized strain on the immediate ligands (in this case, the octahedron of oxygen ions). In effect, what happens could be described in terms of an effective Stark stress that arises through the interaction between a cation with degenerate orbital angular momentum states and the octahedron of charged ligands that provides the crystal field. This stress acts on the octahedron until the increase in elastic energy offsets the reduction in the cation ground state energy caused by the splitting of the orbital degeneracy.

To establish a new equilibrium condition, the increase in elastic strain energy, which has a quadratic (Hooke's law) dependence on strain, must be compensated by the decrease in site stabilization energy, which has a linear dependence on strain. Thus, the change in site deformation stabilization energy density E^{S} with site deformation strain ϵ^{S} may be defined as an electrostatic site stress

$$\sigma^{S} = dE^{S}/d\epsilon^{S} \quad , \tag{2}$$

where E^{S} may also be considered as the work done per unit volume against elastic restoring forces, and σ^{S} becomes the slope of the linear curve and physically would represent the sensitivity of the splitting of the orbital degeneracy in an axial crystal field. Thus, σ^{S} should be

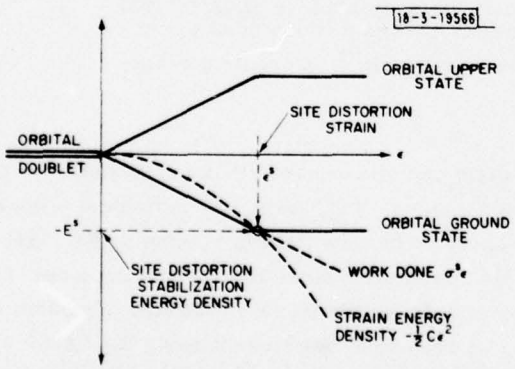

Fig. 6. Crystal-field stabilization energy (Jahn-Teller effect) and its relation to the site distortion strain energy.

considered as a property of the particular cation. To illustrate the relation between the deformation stabilization energy and the strain energy, consider the one-dimensional example shown in Fig. 6. The strain is determined by Hooke's law,

$$\sigma = C\epsilon \quad , \tag{3}$$

where C is Young's Modulus. To balance energy and fix the equilibrium strain experienced by the material, the work done by σ^s must equal the strain energy density E, so that

$$E = \int_0^{\epsilon} \sigma \, d\epsilon = \int_0^{\epsilon} C\epsilon \, d\epsilon = (\tfrac{1}{2}) C\epsilon^2 \quad . \tag{4}$$

The point where the linear curve (representing both the deformation stabilization energy and the work done against elastic restoring forces) intersects the quadratic curve (representing the strain energy) is the final site stabilization energy density E^s resulting from the action of the site stress σ^s that originates from a Jahn-Teller effect. Therefore, the site distortion strain is simply

$$\epsilon^s = \sigma^s/C \tag{5}$$

and the site distortion stabilization energy density is given by

$$E^s = \tfrac{1}{2} C\epsilon^{s2} = \tfrac{1}{2} \sigma^{s2}/C \quad . \tag{6}$$

To express analytically the strains ϵ_i, for anisotropic systems,

$$\epsilon_i = s_{ij}\sigma_j \quad , \tag{7}$$

where s_{ij} represents components of the compliance tensor, and σ_j are the six components of the stress tensor. For cubic symmetry,[21]

$$\begin{aligned}
\epsilon_1 &= s_{11}\sigma_1 + s_{12}\sigma_2 + s_{12}\sigma_3 \\
\epsilon_2 &= s_{12}\sigma_1 + s_{11}\sigma_2 + s_{12}\sigma_3 \\
\epsilon_3 &= s_{12}\sigma_1 + s_{12}\sigma_2 + s_{11}\sigma_3 \\
\epsilon_4 &= s_{44}\sigma_4 \\
\epsilon_5 &= s_{44}\sigma_5 \\
\epsilon_6 &= s_{44}\sigma_6 \quad .
\end{aligned} \tag{8}$$

For a tetragonally distorted octahedron with a uniaxial stress σ^s_{100} along the [001] axis, $\sigma_1 = \sigma_2 = 0$, and $\sigma_3 = \sigma^s_{100}$. Equation (4) yields the following non-zero strains,

$$\begin{aligned}
\epsilon^s_{||} &= \epsilon^s_{001} = s_{11}\sigma^s_{100} \\
\epsilon^s_{\perp} &= \epsilon^s_{010} = \epsilon^s_{100} = s_{12}\sigma^s_{100} \quad ,
\end{aligned} \tag{9}$$

where $\epsilon^s_{||}$ refers to the primary strain (collinear with the direction of the uniaxial stress) and $\epsilon^s_{\perp}$, to the secondary orthogonal strains, which are of smaller magnitude and opposite sign to $\epsilon^s_{||}$.

For a simple cubic host lattice (where every site is octahedral, e.g., MgO), with active ions occupying n out of a total of N sites, a magnetic field along a $\langle 111 \rangle$ direction would divide the n tetragonal site distortions equally among the three $\langle 100 \rangle$ directions. To estimate

the resultant effect on the entire lattice, consider the following definitions

$$\epsilon^s = d\ell/\ell \quad , \quad \lambda = dL/L \quad , \tag{10}$$

where ℓ represents a site dimension, and L, the lattice dimension along the same axis. Since it may be shown that $dL = (n/N^{2/3})\, d\ell$ and $L = N^{1/3}\ell$ in this model,

$$\lambda = f\epsilon^s \quad , \tag{11}$$

where $f = n/N$. With the aid of Eq. (11), an estimate of the resultant lattice strain for $\vec{H} \,||\, [111]$ could be considered as follows:

$$\epsilon^{111}_{001} = f\left(\tfrac{1}{3}\,\epsilon^s_{001} + \tfrac{1}{3}\,\epsilon^s_{010} + \tfrac{1}{3}\,\epsilon^s_{100}\right) \quad , \tag{12}$$

$$= \frac{f}{3}\left(\epsilon^s_{||} + 2\epsilon^s_{\perp}\right) \quad . \tag{13}$$

From Eq. (9), Eq. (13) may be expressed as

$$\epsilon^{111}_{001} = (f/3)\,(s_{11} + 2s_{12})\,\sigma^s_{100} \quad . \tag{14}$$

By the same reasoning, when $\vec{H} \,||\, [001]$, all n site distortions are collinear with $\vec{H}$ and the resultant lattice strain becomes

$$\epsilon^{001}_{001} = f s_{11} \sigma^s_{100} \quad . \tag{15}$$

To determine the magnetostrictive strain along the [001] axis when $\vec{H}$ is rotated from the [111] to the [001] axis, as depicted in Fig. 4, Eq. (14) is subtracted from Eq. (15) to yield

$$\Delta\lambda^{tet}_{100} = \left(\frac{2}{3}\, f\right)(s_{11} - s_{12})\,\sigma^s_{100} \quad . \tag{16}$$

By the symmetry argument used earlier, it was concluded that no first-order strain should appear along the [111] axis, so that

$$\Delta\lambda^{tet}_{100} \simeq 0 \quad . \tag{17}$$

For the case of a site distortion along a $\langle 111 \rangle$ axis, the reasoning is identical to the above, but the analytical solution to the problem is much more tedious because the stress and compliance tensors must be referred to a coordinate system with the c-axis along a $\langle 111 \rangle$ direction. To determine the strain ϵ^s_{111} for a uniaxial stress σ^s_{111}, a quick answer may be obtained by using the general relation for the reciprocal of the Young's Modulus where stress and strain are collinear.[22] For a cubic system

$$C^{-1} = s_{11} - 2(s_{11} - s_{12} - \tfrac{1}{2}\, s_{44})\,(\beta_1^2\beta_2^2 + \beta_2^2\beta_3^2 + \beta_3^2\beta_1^2) \quad . \tag{18}$$

Along the [001] axis, $\beta_1 = \beta_2 = 0$, $\beta_3 = 1$, and $C^{-1} = s_{11}$; along the [111] axis, $\beta_1 = \beta_2 = \beta_3 = 1/\sqrt{3}$ and

$$C^{-1} = \tfrac{1}{3}\,(s_{11} + 2s_{12} + s_{44}) \quad . \tag{19}$$

Thus, the primary site strain becomes

$$\epsilon^s_{||} = \epsilon^s_{111} = \tfrac{1}{3}\,(s_{11} + 2s_{12} + s_{44})\,\sigma^s_{111} \quad . \tag{20}$$

For the contributions from sites distorted along the remaining three $\langle 111 \rangle$ axes (i.e., $[\bar{1}11]$, $[\bar{1}\bar{1}1]$, and $[1\bar{1}1]$), the computation must be carried out in a frame of reference with the c-axis along the [111] direction. If σ^{s}_{111} is along the $[\bar{1}\bar{1}1]$ axis, the stress tensor must undergo a similarity transformation to rotate the c-axis from the $[\bar{1}\bar{1}1]$ direction to the [111] direction and produce new tensor elements. In addition, a similarity transformation from the original cubic axes system to the [111] system must be used to rotate the 4th-rank compliance tensor.[23] The details of this task are too lengthy to reproduce in this text. However, the results of the calculation of the tensor multiplication carried out in the [111] frame of reference for a site distortion along the $[\bar{1}\bar{1}1]$ axis produce the following expression for the secondary contribution to the [111] axis strain:

$$\epsilon^{s}_{\perp} = (0.189s_{11} + 0.671s_{12} - 0.039s_{44})\,\sigma^{s}_{111} \quad . \tag{21}$$

Because site distortions along the $[\bar{1}11]$ and $[1\bar{1}1]$ axes would also produce the secondary strain described by Eq. (21), the contribution to the total strain along the [111] axis from equally distributed site distortions along the other three $\langle 111 \rangle$ axes would triple $\epsilon^{s}_{\perp}$. Since this situation describes the state of strain along the [111] direction when trigonally distorted sites are equally distributed among the four trigonal axes, it also represents the case for the magnetic field $\vec{H} \,||\, [001]$ axis. Thus, with appropriate weighting for primary and secondary contributions, the lattice strain becomes

$$\epsilon^{001}_{111} = (f/4)\,(\epsilon^{s} + 3\epsilon^{s}) \quad , \tag{22}$$

and from Eqs. (20) and (21), Eq. (22) may be expressed as

$$\epsilon^{001}_{111} = (f/4)\,(0.225s_{11} + 0.670s_{12} + 0.054s_{44})\,\sigma^{s}_{111} \quad . \tag{23}$$

When $\vec{H}$ is rotated to the [111] direction, every site distortion will switch to the [111] axis, and the total strain along this axis will be simply the combined effect of n primary trigonal strains, or

$$\epsilon^{111}_{111} = f\epsilon^{s}_{111} = (f/3)\,(s_{11} + 2s_{12} + s_{44})\,\sigma^{s}_{111} \quad . \tag{24}$$

To determine the net magnetostrictive effects from rotation of the magnetic field, all that is required is a subtraction of Eq. (23) from Eq. (24) to yield

$$\Delta\lambda^{trig}_{111} = f(0.108s_{11} - 0.003s_{12} + 0.279s_{44})\,\sigma^{s}_{111} \quad . \tag{25}$$

From the same symmetry argument used earlier,

$$\Delta\lambda^{trig}_{100} \simeq 0 \quad . \tag{26}$$

In Table I, the results for the different situations of tetragonal and trigonal distortions are summarized. The conclusions that $\Delta\lambda_{111} = 0$ for the tetragonal case and $\Delta\lambda_{100} = 0$ for the trigonal case are based on the assumption that cubic symmetry is maintained when the site switching takes place. If the total strain were sufficient to reduce the overall lattice symmetry, the above approximations would no longer be valid. In most cases, however, the magnetostrictive strains are on the order of only a few parts per million.

TABLE I

EFFECTS OF TETRAGONAL AND TRIGONAL OCTAHEDRAL SITE DISTORTIONS ON THE λ_{100} AND λ_{111} MAGNETOSTRICTION CONSTANTS

Site Distortion		$\Delta\lambda_{100}$	$\Delta\lambda_{111}$
Tetragonal	$c/a > 1$	$+\frac{2}{3} f(s_{11} - s_{12}) \lvert\sigma^s_{100}\rvert$	0
	$c/a < 1$	$-\frac{2}{3} f(s_{11} - s_{12}) \lvert\sigma^s_{100}\rvert$	0
Trigonal	$\alpha < 60°$	0	$+f(0.108s_{11} - 0.003s_{12} + 0.279s_{44}) \lvert\sigma^s_{111}\rvert$
	$\alpha > 60°$	0	$-f(0.108s_{11} - 0.003s_{12} + 0.279s_{44}) \lvert\sigma^s_{111}\rvert$

TABLE II

PROPOSED EFFECTS OF TETRAGONAL AND TRIGONAL OCTAHEDRAL SITE DISTORTIONS ON THE λ_{100} AND λ_{111} MAGNETOSTRICTION CONSTANTS FOR A SIMPLE CUBIC LATTICE (e.g., MgO)

Site Distortion		$\Delta\lambda_{100}$	$\Delta\lambda_{111}$
Tetragonal	$c/a > 1$	$3.3 \times 10^{-13} f \lvert\sigma^s_{100}\rvert$	0
	$c/a < 1$	$-3.3 \times 10^{-13} f \lvert\sigma^s_{100}\rvert$	0
Trigonal	$\alpha < 60°$	0	$+2.2 \times 10^{-13} f \lvert\sigma^s_{111}\rvert$
	$\alpha > 60°$	0	$-2.2 \times 10^{-13} f \lvert\sigma^s_{111}\rvert$

For a MgO lattice, the compliance constants may be considered as representative of those for an individual octahedral site. To approximate the stress-strain relationships for octahedral sites, the following MgO values of s_{11}, S_{12}, and s_{44} were used to compute the relations in Table II:[24]

$$s_{11} = 0.400 \times 10^{-12}$$

$$s_{12} = -0.097 \times 10^{-12}$$

$$s_{44} = 0.643 \times 10^{-12} \text{ cm}^2/\text{dyne} \quad . \tag{27}$$

For a garnet or spinel lattice, the presence of tetrahedral and dodecahedral sites may be taken into account in determining the resultant effect on $\Delta\lambda_{100}$ and $\Delta\lambda_{111}$ by defining an effective concentration factor f'. This analysis is presented in the appendix.

III. COMPARISON WITH EXPERIMENT

In order to test the applicability of the local site distortion model, the magnetostriction constant data for octahedral-site Mn^{3+}, Co^{2+}, and Fe^{2+} ions in spinels and garnets will be reviewed. The crystal structures of these host lattices feature a trigonal component to the crystal field ($\sim 10^2$ to 10^3 cm^{-1}) which is about an order of magnitude smaller than the main octahedral field ($\sim 10^4$ cm^{-1}), but considerably larger than the Jahn-Teller deformation energy required to account for the magnetostriction effects (see appendix). The trigonal field is responsible for the anisotropy effects associated with Co^{2+} and Fe^{2+} (Ref. 14), but does not affect the magnetostriction distortion as long as the crystal-field stabilization effects from both sources do not oppose each other. In the case of the Mn^{3+} ion, the trigonal field has no stabilization effect whatsoever, because the Jahn-Teller phenomenon can only result from a tetragonal or orthorhombic distortion. Although the trigonal field does not play a direct role in the local site distortion model of magnetostriction, it will be included in the energy-level diagrams of the individual ions.

A. The Mn^{3+} Ion (High-Spin State)

Trivalent manganese ($3d^4$) in an octahedral site is a pure Jahn-Teller ion, and its ^5D ground orbital term is split into a lower doublet and upper triplet under the influence of a crystal field of six octahedrally coordinated oxygen anions, as shown in Fig. 7. In a trigonal field, the doublet term is not split, but the Jahn-Teller effect may occur in the form of a tetragonal (or orthorhombic) distortion which will stabilize the ion by lifting this degeneracy. According to Goodenough,[13] elastic restoring forces are expected to create an effective distortion (whether static or dynamic) that would favor tetragonal symmetry with $c/a > 1$ (see Fig. 2). This latter conclusion is supported by the fact that when the distortions become cooperative, as in Mn_3O_4, the lattice undergoes a phase change from cubic to tetragonal symmetry. Based on the theoretical conclusions summarized in Table II, $\Delta\lambda_{100}$ is expected to be positive and $\Delta\lambda_{111}$ negligible. As a test for these predictions, consider the garnet data of Dionne[1] presented in Fig. 8 and the spinel data of Van Hook and Dionne[4] given in Fig. 9. In both cases, the λ_{100} constant experiences a significant change in a positive sense, while λ_{111} remains relatively insensitive to the increasing concentration of Mn^{3+} ions. For $Y_3Mn_xFe_{5-x}O_{12}$, the small variation of λ_{111} with x could

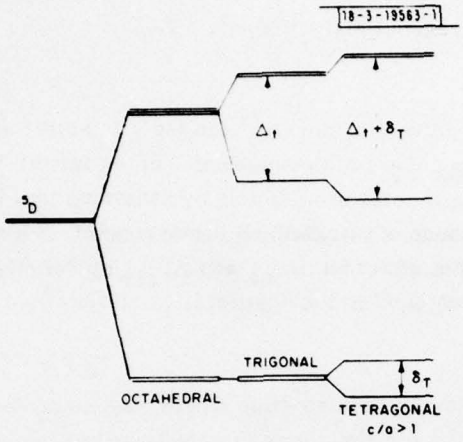

Fig. 7. Crystal-field energy level structure of octahedral-site Mn^{3+} ions in spinel and garnet lattices.

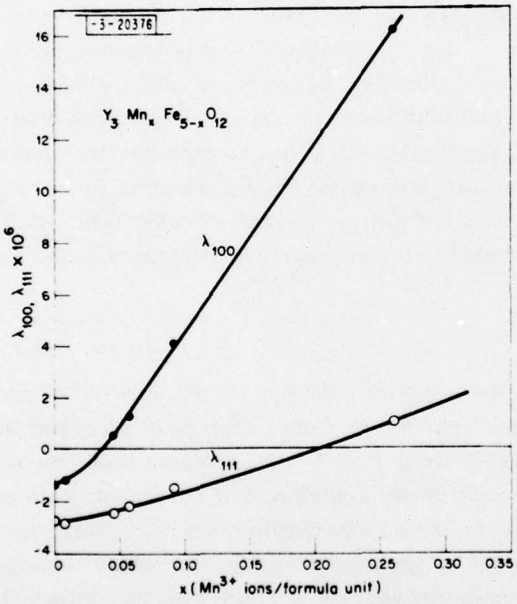

Fig. 8. Variation in the room-temperature magnetostriction constants of yttrium-iron garnet with Mn^{3+} concentration (after Dionne, Ref. 1).

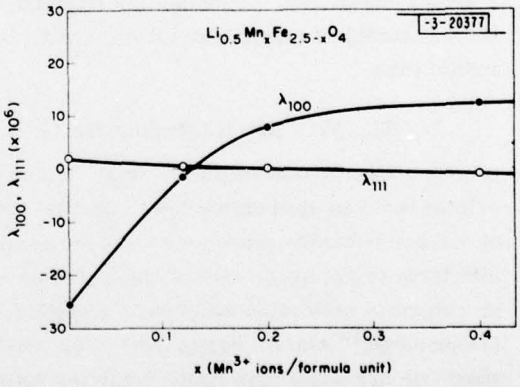

Fig. 9. Variation in the room-temperature magnetostriction constants of lithium ferrite with Mn^{3+} concentration (after Van Hook and Dionne, Ref. 4).

occur because the octahedral site axes are not quite coincident with those of the garnet lattice.[17] It should also be pointed out that the actual Mn^{3+} content in $Li_{0.5}Mn_xFe_{2.5-x}O_4$ may be inaccurate because some fraction of the manganese substitution may have entered the lattice as Mn^{2+} and would not produce Jahn-Teller effects. However, both systems agree precisely with the qualitative predictions of the model for the tetragonal distortion $c/a > 1$.

B. The Co^{2+} Ion (High-Spin State)

In an octahedral site, the ^4F orbital ground term of the Co^{2+} ion ($3d^7$) is split into an upper singlet and a pair of lower triplets by the main cubic field component. In the ferrite hosts, Slonczewski[14] has interpreted the anisotropy and relaxation effects by assuming that the trigonal field component splits the ground triplet into an upper singlet and lower doublet, as shown in Fig. 10. Since this trigonal field is equivalent in sign to a distortion $\alpha > 60°$ according to Goodenough,[25] a tetragonal $c/a < 1$ deformation would produce an additional stabilization, prior

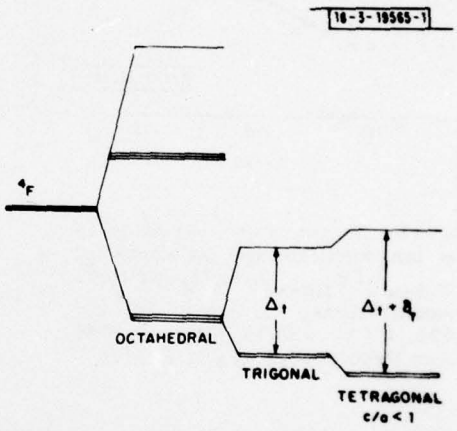

Fig. 10. Crystal-field energy level structure of octahedral site Co^{2+} ions in spinel and garnet lattices.

to the final lifting of the ground orbital degeneracy by spin-orbit coupling. Goodenough's analysis also predicts that elastic restoring forces would more likely favor the $c/a < 1$ deformation below the Néel temperature, and this result has been borne out in CoO. Accordingly, magnetostrictive effects arising from the substitution of small amounts of Co^{2+} ions into octahedral sites should follow the trends indicated in Table II for a $c/a < 1$ distortion.

For a $c/a < 1$ distortion, $\Delta\lambda_{100}$ should be negative and $\Delta\lambda_{111}$ negligible. Unfortunately, the available experimental results for Co^{2+} in the garnet system are sparse and inconclusive.[5] However, Protopopova et al.[6] have reported data on the magnetostriction constants of Co^{2+}-doped lithium and magnesium ferrite as a function of temperature (see Figs. 11 and 12). In both cases, the effects of Co^{2+} are seen to follow qualitatively the theoretical expectations. In addition, Bozorth et al.[7] reported the room-temperature results for Fe_3O_4 and $Co_{0.8}Fe_{2.2}O_4$ presented in Table III, which clearly show how the presence of divalent cobalt can produce a very large negative λ_{100} constant. With the addition of Zn^{2+} and subsequent reduction of the Co^{2+} content in $Co_{0.35}Zn_{0.26}Fe_{2.39}O_4$, the magnitude of λ_{100} decreases accordingly without affecting λ_{111}. A room-temperature measurement of the magnetostriction constants of Co^{2+}-doped lithium ferrite also reveals a small increase in the negative value of λ_{100} (Ref. 2).

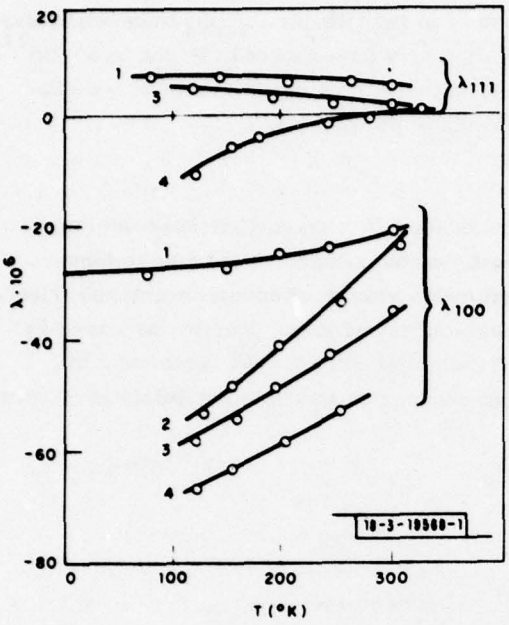

Fig. 11. Temperature variation in the magnetostriction constants of $Li_{0.5-x/2}Fe_{2.5-x/2}Co_xO_4$ for Co^{2+} concentrations: (1) x = 0, (2) x = 0.003, (3) x = 0.0035, (4) x = 0.0044 (after Protopopova et al., Ref. 6).

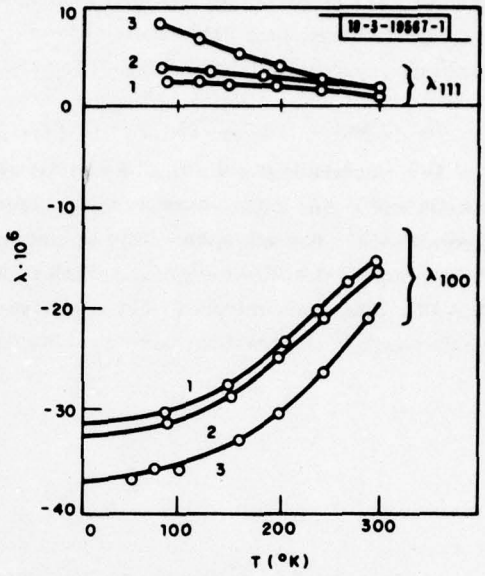

Fig. 12. Temperature variation in the magnetostriction constants of $Mg_{1-x}Co_xFe_2O_4$ for Co^{2+} concentrations: (1) x = 0, (2) x = 0.0002, (3) x = 0.002 (after Protopopova et al., Ref. 6).

TABLE III

MAGNETOSTRICTION CONSTANTS OF SELECTED SPINEL FERRITE COMPOSITIONS CONTAINING Co^{2+} AND Fe^{2+} IONS

Composition	$\lambda_{100} \times 10^{-6}$	$\lambda_{111} \times 10^{-6}$	Reference
$Fe^{3+}_{1.0}[Fe^{3+}_{1.0}Fe^{2+}_{1.0}]O_4$	−19	+81	6
$Fe^{3+}_{1.0}[Co^{2+}_{0.8}Fe^{3+}_{1.0}Fe^{2+}_{0.2}]O_4$	−590	+120	6
$Fe^{3+}_{0.78}Zn^{2+}_{0.22}[Co^{2+}_{0.33}Fe^{3+}_{1.22}Fe^{2+}_{0.45}]O_4$	−210	+110	6
$Fe^{3+}_{1.0}[Li^{1+}_{0.5}Fe^{3+}_{1.5}]O_4$	−25.8	+2.3	2
$Fe^{3+}_{1.0}[Li^{1+}_{0.49}Co^{2+}_{0.02}Fe^{3+}_{1.49}]O_4$	−28.7	+5.0	2

In the work reported by Bozorth et al., all compositions contained substantial amounts of divalent iron ions. As will be discussed next, Fe^{2+} ions are responsible for the large positive values of λ_{111} in these compositions.

C. The Fe^{2+} Ion (High-Spin State)

In an octahedral crystal field, the ^5D ground orbital term of the Fe^{2+} ion ($3d^6$) is split into an upper doublet and lower triplet (the inverse of Mn^{3+}). In the spinel or garnet lattice, the trigonal field will split the lower triplet into a singlet and doublet, but some question exists as to the sign of this splitting. Slonczewski[14] has pointed out that the situation should be the inverse of that for Co^{2+} if the trigonal field is solely the result of long-range effects from the host lattice. This would produce an orbital singlet ground state and would not account for the magnetostrictive effects.

However, Feher and Sturge[26] have concluded that short-range interactions sensitive to local charge compensation may disturb and even override the basic trigonal field component to make the sign of the splitting vary among different cations. In addition, Judy[27] has pointed out that the negative second-order anisotropy constant K_2 of Fe^{2+} measured in $Y_3Fe_5O_{12}$ can only be explained by a doublet ground state. Finally, observed anisotropy and relaxation effects of Fe^{2+} in ferrites are difficult to explain without the aid of spin-orbit stabilization effects, which are expected to be large if the ground state is degenerate. Accordingly, the energy-level model shown in Fig. 13 will be assumed for the interpretation of the magnetostriction data.

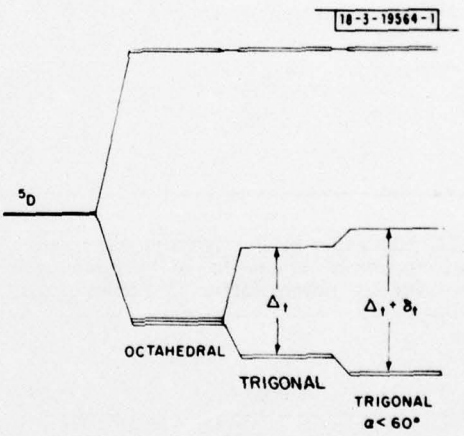

Fig. 13. Crystal-field energy level structure of Fe^{2+} ions in spinel and garnet lattices.

Since the trigonal field depicted would be equivalent to an $\alpha < 60°$ distortion by Goodenough's analysis, a Jahn-Teller deformation of this type would reinforce the crystal-field stabilization prior to the final removal of the orbital degeneracy by spin-orbit coupling. In accord with this prediction, divalent iron in FeO was indicated as an example of such a trigonal ($\alpha < 60°$) distortion at lower temperatures. This result is consistent with the fact that magnetostriction creates weaker elastic restoring forces for this trigonal distortion in contrast to the stronger forces associated with a tetragonal ($c/a > 1$) distortion. As in the case of Co^{2+} in an octahedral site, crystal-field stabilization of the Fe^{2+} ion energy levels is expected to favor one particular type of distortion, and its effects on magnetostriction constants when substituted into a garnet or spinel lattice may be determined through an examination of the existing experimental data.

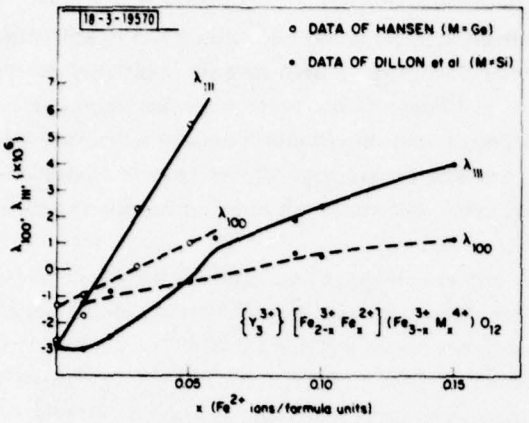

Fig. 14. Variation in the room-temperature magnetostriction constants of yttrium-iron garnet with Fe^{2+} ion concentration (after Dillon et al., Ref. 10 and Hansen, Ref. 11).

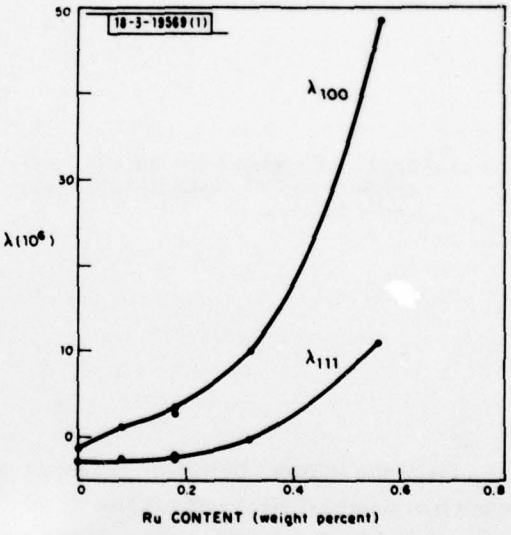

Fig. 15. Variation in the room-temperature magnetostriction constants of yttrium-iron garnet with Ru content (after Krishnan et al., Ref. 28).

According to the theoretical results summarized in Table II, Fe^{2+} ions with an $\alpha < 60°$ distortion should provide a positive $\Delta\lambda_{111}$ and a negligible $\Delta\lambda_{100}$. In Fig. 14, the magnetostriction constant measurements of Fe^{2+} in yttrium iron garnet reported by Dillon et al.[10] and Hansen[11] are reproduced in order to verify the qualitative agreement with the model. The differences in the two sets of data suggest discrepancies in the determinations of Fe^{2+} ion concentrations. For the spinel lattice, Table III reveals the large positive λ_{111} constant of Fe_3O_4 and the generally high values of this quantity in the Co ferrite compositions, which also contain large amounts of divalent iron.

In general, all of the available experimental results are in complete accord with the qualitative predictions of the magnetostriction model and are consistent with the type of octahedral site distortion predicted from crystal-field theory. In addition to the three ions studied, other possibilities exist, but limited experimental results are available. Two such candidates are Ru of the 4d transition series and Ir of the 5d series. Under certain crystal-field conditions, ions of both of these elements can behave in a manner similar to Co^{2+} or Fe^{2+} in an octahedral site and significant magnetostriction constant changes could occur. For example, Krishnan et al.[28] have reported magnetostriction measurements of Ru^{3+} ($4d^5$) or Ru^{4+} ($4d^4$) ions in yttrium iron garnet which behave analogously to Mn^{3+} ions in the same lattice (see Fig. 7). Because of the larger spatial extent of the 4d wave functions, the effective intensity of the octahedral crystal field is great enough to place these ions in low-spin states with orbital triplet ground states. Crystal field and spin-orbit stabilization would be anticipated in these cases. From the data in Fig. 15, it appears that a local tetragonal ($c/a > 1$) deformation similar to that of Mn^{3+} probably takes place for the particular Ru ion investigated.

IV. DISCUSSION AND CONCLUSIONS

The local site distortion model proposed to explain the magnetostrictive effects of small concentrations of selected transition-metal ions in spinel and garnet lattices has been demonstrated to be capable of interpreting the changes in either the λ_{100} or the λ_{111} magnetostriction constant on a qualitative basis. In every instance reviewed, the theoretical predictions are in qualitative agreement with experimentally determined changes in magnetostrictive constants as a function of concentration. In addition, the particular types of deformation required to fit the data are in accord with those expected from crystal-field and elastic restoring force considerations. Observed changes in the second magnetostriction constant are not predicted by this model, but may be partially accounted for by the fact that the volume of the lattice was assumed to be unchanged during magnetostriction. Any departure from this idealized situation could produce small changes in the second constant. In addition, indirect effects of the substituted cations on the magnetostrictive contributions from the host Fe^{3+} ions were not considered.

In the theory described in this paper, a pure octahedral crystal-field environment was assumed for the development of the model. In reality, spinel and garnet lattices feature a significant trigonal component of the field, directed along one of the four $\langle 111 \rangle$ axes at each octahedral site. This field component accounts for the anisotropy effects characteristic of these ferrimagnetic materials and the question of what influence this field component could have on the basic model should now be considered. Because the site distortions are Jahn-Teller effects arising from the tendency of the ion to lower the energy of its ground state by a deformation of its immediate ligands, the presence of the other crystal-field components should not in themselves affect these distortions as long as the conditions necessary for their occurrence are sustained.

In the absence of a magnetic field, the crystal-field splittings of the respective ions are sketched in Figs. 7, 10, and 13, where it is indicated that small Jahn-Teller stabilizations can take place in each case; the signs of the distortions are such as to enhance the effects of the trigonal field. For the Mn^{3+} ion case shown in Fig. 7, the trigonal field does not affect the ground orbital doublet and may therefore be treated as nonexistent. In the presence of a magnetic field, the symmetry axes of each local site distortion will follow the magnetic field direction in spite of the fixed trigonal field component along a specific ⟨111⟩ axis. For Co^{2+} ions, the distortion is tetragonal along any one of the three ⟨100⟩ directions. Therefore, each of these axes is symmetrically and energetically equivalent with respect to the trigonal field. Whether the magnetic field is directed along a ⟨100⟩ axis or a ⟨111⟩ axis, all of the site distortions will remain along ⟨100⟩ axes and the basic concept of site switching among ⟨100⟩ directions as the field is rotated is valid. However, in the presence of anisotropy fields, an activation energy or critical magnetic field strength for saturation may exist to effect the necessary switching.

The case of Fe^{2+} ions is less obvious because both crystal-field components are trigonal and directed along ⟨111⟩ axes. With the magnetic field along a ⟨100⟩ axis, each site distortion would align with the fixed trigonal field direction for the particular site in a manner equivalent to the zero-field case depicted in Fig. 5. However, with the field along a ⟨111⟩ axis, the site distortions are not equivalent and three out of four of the distortions must switch to a new ⟨111⟩ direction 70.5° from their fixed trigonal field axes. Since the axis of the site distortion will follow the orbital angular momentum vector, the phenomenon depicted in Fig. 1 should take place, as $\vec{H}$ will rotate $\vec{S}$, which in turn is coupled to $\vec{L}$ through spin-orbit coupling. Because it is through the competition between crystal field and magnetic field for the $\vec{L}$ vector that the magnetocrystalline anisotropy energy originates, it is logical that the system would lower its energy by reducing the crystal-field strength through a site distortion switch over to the direction of the magnetic field. Once again, questions of a saturation field strength required to overcome anisotropy arise, but the essence of the argument resides in the notion that the system will eventually attain its greatest spin-orbit stabilization with all the site distortions directed along the ⟨111⟩ axis closest to the magnetic field direction. This last argument will apply to any situation where part of the axial crystal field is switchable through a local site distortion, without disturbing the fixed field of the host lattice, and would also apply to the magnetostrictive changes caused by Mn^{3+} and Co^{2+} ions discussed above.

From the above discussion, it may be concluded that the local site distortion switching concept of magnetostriction is valid in the presence of non-cubic crystal-field components. It should also be pointed out that the presence of an internal magnetization or exchange field is not required, although all data discussed were derived from measurements on ferrimagnetic materials. The existence of Jahn-Teller effects from Co^{2+} ions in MgO (Ref. 29) and $Y_3Ga_5O_{12}$ (Ref. 30) have not been detected by paramagnetic resonance at 4.2 K, but such distortions may be the cause of a line broadening with Fe^{2+} ions in MgO (Ref. 31). However, unless crystal-field energies are much greater than 10^{-2} cm^{-1} (see appendix) at liquid-helium temperature, such effects may not be discernible by resonance spectroscopy techniques, and actual magnetostriction measurements may be required to investigate the possibility that paramagnetic materials may possess magnetostrictive properties.

ACKNOWLEDGMENTS

The author is indebted to Professor John B. Goodenough of Oxford University for providing insight into some of the crystal-field phenomena intrinsic to the model, Russell G. West of Trans-Tech, Inc., and Dr. Geoffrey O. White of Colorado State University for calling attention to magnetostriction constant data pertinent to this work.

REFERENCES

1. G. F. Dionne, IEEE Trans. Magnetics MAG-7, 715 (1971), DDC AD-737934.
2. G. F. Dionne, J. Appl. Phys. 40, 4486 (1969), DDC AD-703756.
3. G. F. Dionne, J. Appl. Phys. 41, 831 (1970), DDC AD-707583.
4. H. J. Van Hook and G. F. Dionne, Mag. and Mag. Matls. AIP Conf. Proc. No. 24, 487 (1975).
5. G. F. Dionne and J. B. Goodenough, Mater. Res. Bull. 7, 749 (1972), DDC AD-752994.
6. L. M. Protopopova, G. A. Petrakovskii, and E. V. Rubal'skaya, Bull. Acad. Sci. USSR 36, 1110 (1972).
7. R. M. Bozorth, E. F. Tilden, and A. J. Williams, Phys. Rev. 99, 1788 (1955).
8. P. Hansen, W. Tolksdorf, and J. Schuldt, J. Appl. Phys. 43, 4740 (1972).
9. D. R. Mack and J. Smit, Appl. Phys. 2, 23 (1973).
10. J. F. Dillon, Jr., E. M. Gyorgy, and J. P. Remeika, Appl. Phys. Lett. 9, 147 (1966).
11. P. Hansen, J. Appl. Phys. 48, 801 (1977).
12. J. B. Goodenough, The Molecular Designing of Materials and Devices (MIT Press, Cambridge, Massachusetts, 1965), p. 42.
13. J. B. Goodenough, Magnetism and the Chemical Bond (Interscience-Wiley, New York, 1963).
14. J. C. Slonczewski, J. Appl. Phys. 32, 253S (1961).
15. J. H. Van Vleck, Discuss. Faraday Soc. No. 26, 96 (1958).
16. F. Euler and J. A. Bruce, Acta. Cryst. 19, 971 (1965).
17. G. F. Dionne, J. Appl. Phys. 40, 1839 (1969), DDC AD-694193.
18. H. A. Jahn and E. Teller, Proc. Roy. Soc. (London) A161, 220 (1937).
19. L. E. Orgel, Introduction to Transition-Metal Chemistry (Wiley, New York, 1966).
20. J. H. Van Vleck, J. Chem. Phys. 7, 72 (1939).
21. J. F. Nye, Physical Properties of Crystals (Oxford University Press, London, 1960), p. 143.
22. Ibid., p. 145.
23. W. L. Bond, Bell Syst. Tech. J. 22, 1 (1943).
24. D. H. Chung, "Selected Materials for Use in Microsound Circuits and Components: Their Elastic, Piezoelectric, and Dielectric Parameters," Technical Note 1969-29, Lincoln Laboratory, M.I.T. (8 May 1969), DDC AD-692111.

25. J.B. Goodenough, Phys. Rev. 171, 466 (1968), DDC AD-677856.

26. E. Feher and M. D. Sturge, Phys. Rev. 172, 244 (1968).

27. J. H. Judy, J. Appl. Phys. 37, 1328 (1966).

28. R. Krishnan, V. Cagan, and M. Rivoire, Mag. and Mag. Matls. AIP Conf. Proc. No. 5, 704 (1972).

29. W. Low, Phys. Rev. 109, 256 (1958).

30. M. D. Sturge, F. R. Merritt, J. C. Hensel, and J. P. Remeika, Phys. Rev. 180, 402 (1969).

31. W. Low, Paramagnetic Resonance in Solids (Academic Press, New York, 1960), p. 89.

APPENDIX

A. MULTI-SITED LATTICE

For a multi-sited lattice, e.g., $Y_3Fe_5O_{12}$ with octahedral, tetrahedral, and dodecahedral sites in the ratio of 2:3:3, a linear dimension ℓ_i of a particular site can be estimated from its volume v_i by $\ell_i \simeq v_i^{1/3}$.

Then,

$$d\ell_i = \epsilon^s \ell_i \simeq \epsilon^s v_i^{1/3} \quad ,$$

and

$$L = V^{1/3} \quad , \tag{A-1}$$

where V is the volume of the lattice. Since

$$dL = (n_i/N^{2/3})\, d\ell_i \simeq \epsilon^s (n_i/N^{2/3})\, v_i^{1/3} \tag{A-2}$$

$$\epsilon = dL/L \simeq \epsilon^s (n_i/N^{2/3})\, (v_i/V)^{1/3} \quad . \tag{A-3}$$

However, since V = Nv, where v is the mean site volume,

$$\epsilon \simeq \epsilon^s (n_i/N)\, (v_i/v)^{1/3} = \epsilon^s f_i (v_i/v)^{1/3} \quad . \tag{A-4}$$

Thus, Eq. (A-4) may be re-expressed as

$$\epsilon = f_i' \epsilon^s \tag{A-5}$$

where

$$f_i' = f_i (v_i/v)^{1/3} \quad . \tag{A-6}$$

As examples of the types of calculations that may be encountered, consider the garnet and spinel lattices. In both cases, the volume of an octahedral site is approximately 16 A^3. To arrive at values for the mean site volume v, the volume of a unit cell may be determined from the lattice parameters $a_o \sim 12.5$ A for a garnet and ~8.5 A for a spinel. In either case, N would be the total number of cations per unit cell, 64 for the garnet and 24 for the spinel. Therefore,

$$(v_i/v)^{1/3} \simeq 0.81 \text{ (garnet)} \quad ; \quad 0.86 \text{ (spinel)} \quad . \tag{A-7}$$

B. MAGNITUDE OF $\delta_{t,T}$

Because the Jahn-Teller effect represents a crystal-field component that competes with both the host lattice cubic crystal field (octahedral plus trigonal in the case of spinels or garnets) and spin-orbit coupling, it is instructive to estimate the order of magnitude of the site deformation energy density E^s and Jahn-Teller splitting $\delta_{t,T}$. From Eq. (6),

$$E^s = (1/2)\, C \epsilon^{s2} \quad , \tag{A-8}$$

where C is an effective compliance constant. For an individual site, the above relation is valid, provided that estimates may be made for ϵ^s from the relation $\epsilon^s = \epsilon/f_i'$. Thus,

$$E^s = (1/2)C\ (\epsilon/f_i')^2 = (1/2)C\ (\Delta\lambda/f_i')^2 \quad . \tag{A-9}$$

As a typical example, consider the Mn^{3+} ion in $Y_3Fe_5O_{12}$ (Fig. 8). From data presented in the text, it may be determined readily that $C \sim 10^{12}$ dyne/cm^2 and that $\Delta\lambda_{100} \sim 2 \times 10^{-5}$ for $f_i' \simeq 0.024$. Therefore, it may be computed directly from Eq. (A-9) that

$$E^s \sim 3.5 \times 10^5 \text{ ergs/cm}^3 \quad . \tag{A-10}$$

For an octahedral site of volume 16 A^3, the crystal-field energy level splitting δ_t(trigonal) or δ_T(tetragonal) would be on the order of 5.5×10^{-18} ergs, or

$$\delta_{t,T} \sim 3 \times 10^{-2} \text{ cm}^{-1} \quad . \tag{A-11}$$

Since Δ_t from the fixed trigonal crystal field is on the order of 10^2 to 10^3 cm^{-1}, and spin-orbit coupling energy is generally about 10^2 cm^{-1} for these ions, it must be concluded that the local site distortions would be expected to have negligible effect on magnetocrystalline anisotropy.

C. MAGNITUDES OF σ^s_{100}, σ^s_{111}

From Eq. (5), it is assumed that

$$\sigma^s \simeq C\epsilon^s = C(\epsilon/f_i') = C(\Delta\lambda/f_i') \quad . \tag{A-12}$$

For Mn^{3+} ions in $Y_3Fe_5O_{12}$, the values of $C \sim 10^{12}$ dynes/cm^2, $\Delta\lambda_{100} \sim 2 \times 10^{-5}$, and $f_i' \simeq 0.024$ used in the earlier determination of E^s may be applied here to obtain

$$\sigma^s_{100}(Mn^{3+}) \simeq 8.3 \times 10^8 \text{ dynes/cm}^2 \quad . \tag{A-13}$$

For the case of Fe^{2+} ions in $Y_3Fe_5O_{12}$, $C \sim 10^{12}$ dyne/cm^2, $\Delta\lambda_{111} \sim 8 \times 10^{-6}$, and $f_i' \simeq 0.005$ (derived from Hansen data in Fig. 14), and

$$\sigma^s_{111}(Fe^{2+}) \simeq 1.6 \times 10^9 \text{ dynes/cm}^2 \quad . \tag{A-14}$$

☆U. S. GOVERNMENT PRINTING OFFICE: 1979 ⊙ 600-002/27

UNCLASSIFIED

SECURITY CLASSIFICATION OF THIS PAGE *(When Data Entered)*

REPORT DOCUMENTATION PAGE

READ INSTRUCTIONS BEFORE COMPLETING FORM

1. REPORT NUMBER: ESD-TR-78-292	2. GOVT ACCESSION NO.
3. RECIPIENT'S CATALOG NUMBER	
4. TITLE *(and Subtitle)*: Local Site Distortion Model of Magnetostriction	5. TYPE OF REPORT & PERIOD COVERED: Technical Report, TR-
6. PERFORMING ORG. REPORT NUMBER: Technical Report 532	
7. AUTHOR(s): Gerald F. Dionne	8. CONTRACT OR GRANT NUMBER(s): F19628-78-C-0002
9. PERFORMING ORGANIZATION NAME AND ADDRESS: Lincoln Laboratory, M.I.T. P.O. Box 73 Lexington, MA 02173	10. PROGRAM ELEMENT, PROJECT, TASK AREA & WORK UNIT NUMBERS: Project No. 8X363304D215
11. CONTROLLING OFFICE NAME AND ADDRESS: Ballistic Missile Defense Program Office Department of the Army 5001 Eisenhower Avenue Alexandria, VA 22333	12. REPORT DATE: 29 November 1978 13. NUMBER OF PAGES: 28
14. MONITORING AGENCY NAME & ADDRESS *(if different from Controlling Office)*: Electronic Systems Division Hanscom AFB Bedford, MA 01731	15. SECURITY CLASS. *(of this report)*: Unclassified 15a. DECLASSIFICATION DOWNGRADING SCHEDULE

16. DISTRIBUTION STATEMENT *(of this Report)*

Approved for public release; distribution unlimited.

17. DISTRIBUTION STATEMENT *(of the abstract entered in Block 20, if different from Report)*

18. SUPPLEMENTARY NOTES

None

19. KEY WORDS *(Continue on reverse side if necessary and identify by block number)*

magnetostriction
trigonal symmetry
tetragonal symmetry
ferrimagnetic spinels
ferrimagnetic garnets
Jahn-Teller effects
local site distortion

20. ABSTRACT *(Continue on reverse side if necessary and identify by block number)*

A new model is proposed to explain the magnetostriction effects in ferrimagnetic spinels and garnets with Mn^{3+}, Co^{2+}, and Fe^{2+} ions substituted into octahedral sites. Considerable experimental evidence has revealed that small amounts of each of these ions will alter substantially the magnitude of either the λ_{100} or λ_{111} magnetostriction constant, depending on the particular ion. The theory is based on the concept that Jahn-Teller effects produce local site distortions of tetragonal (favoring $\langle 100 \rangle$ axes) or trigonal (favoring $\langle 111 \rangle$ axes) symmetry which are able to switch among the different axes of the particular family in order to select the axis closest to the direction of the magnetic field. For Mn^{3+} ions, the local site distortions are expected to be tetragonal ($c/a > 1$), in accord with observations in a variety of magnetic oxides where static cooperative effects are present, and will produce large positive changes in the λ_{100} constant. With Co^{2+} ions the distortion is also tetragonal, but of the opposite sign ($c/a < 1$), consistent with cooperative effects in CoO, and will produce large negative changes in λ_{100}. In the case of Fe^{2+} ions, the distortion is trigonal ($\alpha < 60°$), as evidenced by its behavior in FeO, and will produce large positive changes in the λ_{111} constant. In each case studied, the theoretical results are in complete accord with the available room temperature magnetostriction constant data on a qualitative basis. An estimate of the magnitude of the elastic energy of the local site distortion suggests that crystal field energy level splittings required to create the observed magnetostrictive effects are only on the order of 10^{-2} cm^{-1}.

DD FORM 1 JAN 73 1473 EDITION OF 1 NOV 65 IS OBSOLETE

20765

UNCLASSIFIED

SECURITY CLASSIFICATION OF THIS PAGE *(When Data Entered)*